Pyrrole-Imidazole Polyamides for Gene Therapy: Bioanalytical Methods and Pharmacokinetics

Tomonori Kamei[1], Takahiko Aoyama[1], Takahiro Ueno[2],
Noboru Fukuda[2,3], Hiroki Nagase[3,4] and Yoshiaki Matsumoto[1]
[1]Department of Clinical Pharmacokinetics, School of Pharmacy, Nihon University
[2]Department of Medicine, Division of Nephrology and Endocrinology
Nihon University School of Medicine
[3]Advanced Research Institute for the Science and Humanities, Nihon University
[4]Division of Cancer Genetics, Department of Advanced Medical Science
Nihon University School of Medicine
Japan

1. Introduction

Pyrrole(Py)-imidazole(Im)(PI) polyamides are small synthetic molecules composed of aromatic rings of *N*-methylpyrrole and *N*-methylimidazole amino acids (Trauger et al., 1996). Synthetic polyamides recognize and bind to specific nucleotide sequences in the minor groove of double-helical DNA with high affinity (Pilch et al., 1996). Various sequence-specific DNA-binding PI polyamides have been developed to regulate gene expression by targeting the promoter regions of enhancer and transcription factor-binding elements in vitro (Murty et al., 2004). PI polyamides were first identified from duocarmycin A and distamycin A, which bind in the minor groove of DNA (Tao et al., 1999; Trauger et al., 1996). Sequence-specific DNA recognition by PI polyamide depends on the sequence of side-by-side amino acid pairs. A pair of Py opposite Im targets the CG base pair, whereas Im opposite Py recognizes the GC base pair, and the Py/Py combination binds to both AT and TA base pairs (White et al., 1997). PI polyamides designed to bind to the transcription factors Ets-1, lymphoid-enhancer binding factor 1, and the TATAbox-binding protein DNA binding site have been shown to inhibit virus replication in isolated human peripheral blood lymphocytes (Dickinson et al., 1998).

PI polyamides can easily enter into the nucleus and bind to chromosomal DNA. Many promising observation for gene therapy using PI polyamides have been reported. PI polyamide targeting rat transforming growth factor (TGF)-β_1 has been reported to inhibit the expressions of TGF-β_1 mRNA and protein in the renal cortex of Dahl-S rats. The targeted PI polyamide also reduced glomerulosclerosis and interstitial fibrosis without side effects. These observations indicate that PI polyamides will be effective for TGF-β_1-related diseases, including progressive renal injury (Matsuda et al., 2011; Matsuda et al., 2006). PI polyamides targeting human aurora kinase-A (AURKA) and -B (AURKB) promoters significantly inhibited the promoter activities, and mRNA and protein expression levels of AURKA and

AURKB. They also demonstrated a marked antiproliferative synergy in human tumor cell lines as a result of induction of apoptosis-mediated severe catastrophe of cell-cycle progression (Takahashi et al., 2008). PI polyamides specifically inhibited lectin-like oxidized low-density lipoprotein receptor-1 mRNA expression and apoptosis induced by oxidized low-density lipoprotein and angiotensin II in human umbilical vein endothelial cells (Ueno et al., 2009). From these observations, PI polyamides have been identified as novel candidates for gene therapy.

Pharmacokinetics is the science that studies the behavior of a circulating drug administered to a body, mainly focusing on absorption, distribution, metabolism, and excretion (ADME) of a drug (Jang et al., 2001). The concentration of a drug in a body can be obtained by a bioanalytical method which includes sample extraction and detection of a drug, and the obtained data are analyzed to evaluate the pharmacokinetics of the drug. Needless to say, a robust bioanalytical procedure is crucial for evaluating the appropriate pharmacokinetic profile of a drug.

In this chapter, we show the bioanalytical procedure, pharmacokinetics, and modeling of PI polyamides A and B. PI polyamides A and B are illustrated in Fig. 1. PI polyamide A was composed of Ac-ImPyPy-ImPyPy-β-Dp (β, β-alanine; Dp, N, N-dimethylaminopropylamide). PI polyamide B was composed of Ac-PyPy-β-PyImPy-PyPyPy-β-ImPy-β-Dp. The molecular weights of PI polyamides A and B were calculated from the sum of the standard atomic weights of all the atoms (Wieser, 2006). The molecular weights of PI polyamides A and B are 1035.12 and 1665.78, respectively. PI polyamide B was designed to bind to the activator protein-1 (AP-1)-binding site of the TGF-β_1 promoter, whereas PI polyamide A also, with a hairpin structure, was designed for comparing with other types of PI polyamide with a hairpin structure and a higher molecular weight.

PI polyamide A
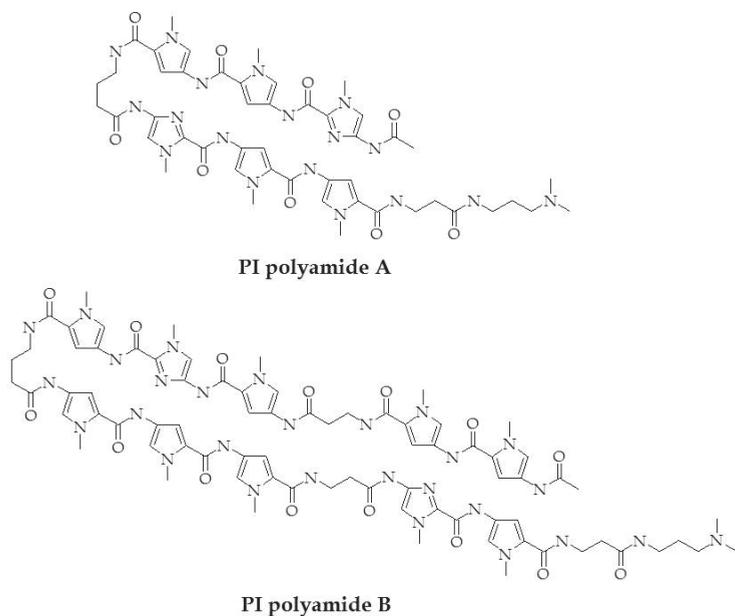
PI polyamide B

Fig. 1. Chemical structures of PI polyamides A and B.

2. Bioanalytics

High-performance liquid chromatography (HPLC) has been used for many years as a useful and conventional tool for the analysis of a drug. Bioanalytical methods by HPLC with UV detection were developed for the determination of PI polyamides A and B in the rat matrix. Sample extraction is one of the important steps and key to success in constructing a robust method. A simple protein precipitation method was developed for the extraction of PI polyamides A and B from rat plasma, whereas solid phase extraction was carried out to extract PI polyamides A and B from rat urine and bile, because a large number of urinary and biliary matrices can interfere with the compounds. It is important to determine the rates of urinary and biliary excretions because these excretions play pivotal roles in the elimination pathway of a drug. The developed methods were successively validated for selectivity, sensitivity, linearity, accuracy, and precision, following the guideline for Bioanalytical Method Validation published by Food and Drug Administration in 2001.

Chromatographic separation was conducted using a reversed-phase TSK-GEL ODS-80T$_M$ (4.6 mm x 150 mm) column maintained at 40 °C. The mobile phase of solvent A was 0.1% acetic acid and that of solvent B was acetonitrile (a linear increase from 0 to 80% B over 10 min (plasma and urine) or 35 min (bile) and an isocratic flow at 60% B for 5 min). The flow rate was set at 1.0 mL/min (plasma and urine) or 0.75 mL/min (bile). The detection wavelength was set at 310 nm. PI polyamides A and B were well separated from the coextracted material under the described chromatographic conditions at approximate retention times of 9.7 (25.0 in bile) and 10.5 min, respectively. The peak shapes were satisfactory and completely resolved from one another. No interference from rat matrices was observed (Fukasawa et al., 2007).
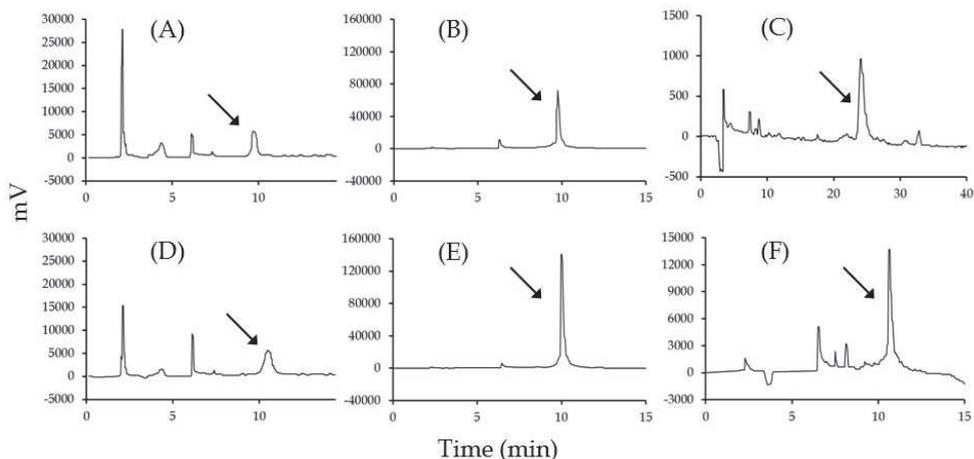
Fig. 2. Representative chromatograms of blank rat plasma (A), blank rat urine (B) and blank rat bile (C) spiked with PI polyamide A, and blank rat plasma (D), blank rat urine (E) and blank rat bile (F) spiked with PI polyamide B. The concentrations of PI polyamides were 5 (A), 20 (B), 1 (C), 5 (D), 20 (E) and 5 (F) μg/mL.

Table 1 shows the intra- and inter-assay precision and accuracy of PI polyamides A and B. The intra- and inter-assay accuracies (RE) were within ± 20% for the lower limit of

quantitation (LLOQ) and ± 15% for the other QC samples. The intra- and inter-assay precisions (CV) were also within the acceptable ranges of 20% for the LLOQ and 15% for the other QC samples. The LLOQ was determined as 1 μg/mL for both PI polyamides A and B. All of the methods were successfully applied to evaluate the pharmacokinetics of the PI polyamides (Fukasawa et al., 2009; Fukasawa et al., 2007; Nagashima et al., 2009b).

Matrix		Nominal concentration (μg/mL)	Intra-assay		Inter-assay	
			RE (%)	CV (%)	RE (%)	CV (%)
Plasma	PI polyamide A	1	2.2	5.3	6.7	14.4
		20	1.4	1.4	-8.7	9.7
		100	7.7	3.7	3.6	3.5
	PI polyamide B	1	2.8	10.0	2.2	15.0
		20	-2.5	0.6	-9.2	7.9
		100	3.7	2.6	3.2	3.2
Urine	PI polyamide A	1	13.4	1.2	4.6	7.9
		20	-0.9	0.7	-4.7	3.6
		200	0.4	0.3	-2.6	4.5
	PI polyamide B	1	7.3	1.9	11.9	4.4
		10	1.9	1.2	0.1	2.3
		20	0.4	0.5	0.1	0.8

Table 1. Intra- and inter-assay accuracy and precision for the determination of PI polyamides A and B in rat plasma and urine.

Although HPLC with UV detection is a useful tool for the determination of a drug, the sensitivity is a limitation factor for evaluating pharmacokinetic characteristic for many hours. Recently, liquid chromatography-tandem mass spectrometry (LC-MS/MS) has been used for the determination of a drug, especially when a sensitivity higher than that of HPLC is required. A bioanalytical method for the determination of PI polyamide A in rat plasma was successfully developed and validated by ultra-performance liquid chromatography (UPLC)-MS/MS with electrospray ionization (Nagashima et al., 2009a).

An MS scan was conducted in the positive ion mode to obtain the precursor ion of PI polyamide A. The mass spectra of PI polyamide A showed significant ions at the *m/z* of 1036, 519, and 346, which corresponds to $[M+H]^+$, $[M+2H]^{2+}$, and $[M+3H]^{3+}$, respectively (Fig. 3). The doubly charged polyamide showed the highest sensitivity during ionization. The product ion spectra of the doubly charged PI polyamide A are shown in Fig. 4. The multiple reaction monitoring (MRM) transition was selected at the *m/z* of 519 and 288.

Chromatographic separation was performed using an ACQUITY UPLC HSS T3 (1.8 μm, 2.1×50 mm) column with an in-line filter and maintained at 40 °C. The liquid flow rate was set at 0.3 mL/min. The mobile phase of solvent A was acetonitrile/water/acetic acid (5/95/0.1, v/v/v) and that of solvent B was acetonitrile/water/acetic acid (95/5/0.1, v/v/v). The gradient started at the mobile phase A-B (95:5%), changed linearly to A-B (45:55%) until 2 min, washed with A-B (0:100%) until 3.5 min, and equilibrated under the initial condition until 5.5 min. PI polyamide A was well separated from the coextracted material under the described conditions at an approximate retention time of 1.5 min. No interference from rat matrices was observed (Fig. 5).
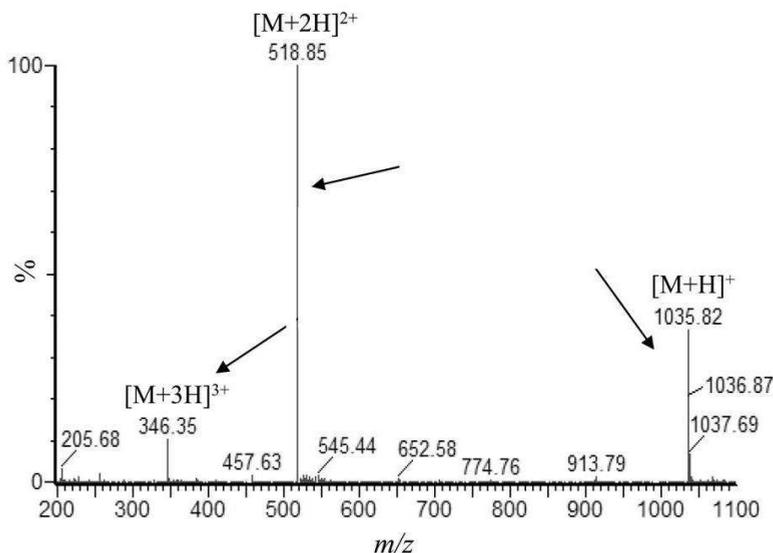
Fig. 3. Representative mass spectra of precursor ions (m/z, 1036 [M+H]+, 519 [M+2H]2+, and 346 [M+3H]3+) of PI polyamide A.
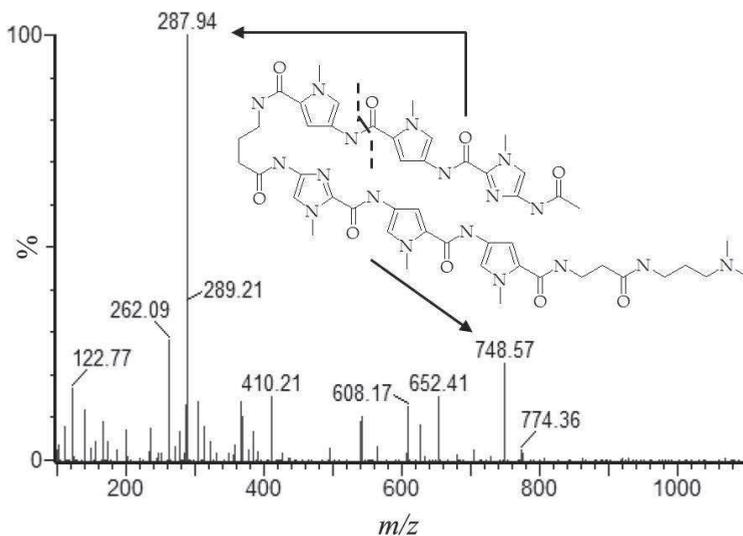
Fig. 4. Representative product ion mass spectra (m/z, 519) of PI polyamide A.

Table 2 shows the intra- and inter-assay precision and accuracy of PI polyamide A. The intra- and inter-assay accuracies (RE) were within ± 20% for the LLOQ and ± 15% for the other QC samples. The intra- and inter-assay precisions (CV) were also within the acceptable ranges of 20% for the LLOQ and 15% for the other QC samples. The LLOQ was

10 ng/mL, which means it has a sufficient sensitivity to evaluate the pharmacokinetics of PI polyamides.
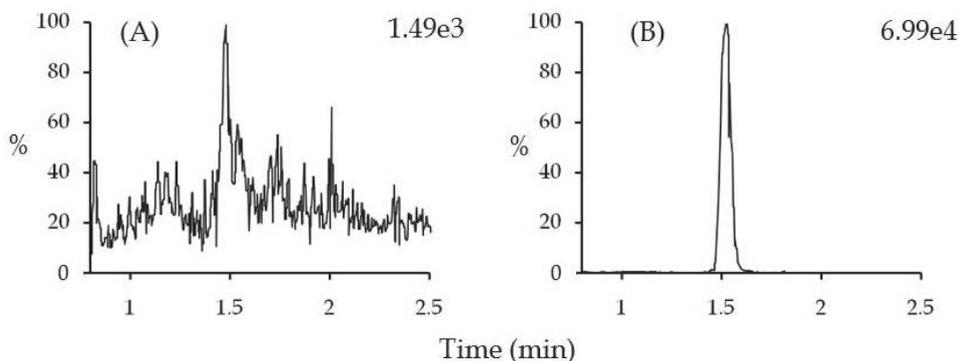
Fig. 5. Representative MRM chromatograms (*m/z*, 519>288) of (A) blank rat plasma, (B) blank rat plasma spiked with PI polyamide A (10 ng/mL).

Nominal concentration	Intra-assay		Inter-assay	
(ng/mL)	RE (%)	CV (%)	RE (%)	CV (%)
10	-10.6	3.3	3.7	11.2
1000	-11.7	1.5	-2.1	9.2
10000	-0.6	4.6	-5.0	8.9

Table 2. Intra- and inter-assay accuracy and precision for the determination of PI polyamide A in rat plasma.

3. Pharmacokinetics of PI polyamides A and B

3.1 Plasma and lung concentrations of PI polyamides A and B

PI polyamide B significantly inhibited the expressions of TGF-β_1 mRNA and protein in the renal cortex of the Dahl-S rats and reduced the rates of increases in the amounts of urinary protein and albumin in the Dahl-S rats independent of blood pressure at a dose of 1.0 mg (Matsuda et al., 2006). From these observations, the doses of PI polyamides were selected on the basis of 1.0 mg dose of PI polyamide B per rat (about 3.0 mg/kg). PI polyamide B had a lower water solubility than PI polyamide A. The doses of PI polyamides A and B were determined to be in the ranges of 1.3-15.0 mg/kg and 1.0-5.0 mg/kg, respectively.

The mean plasma concentration-time profiles after the intravenous administration of PI polyamide A at 1.3, 2.0, 7.5, and 15.0 mg/kg and after that of PI polyamide B at 1.0, 2.0, 3.0, and 5.0 mg/kg are shown in Fig. 6. The plasma concentrations of PI polyamides A and B declined in a polyexponential manner for the four doses studied. The plasma concentration-time profiles of PI polyamides were analyzed by a non-compartmental method. The area under the plasma concentration-time curve ($AUC_{(0-Tlast)}$) and the area

under the first moment curve ($AUMC_{(0-Tlast)}$) were obtained using the linear trapezoidal rule. $AUC_{(Tlast-\infty)}$ and $AUMC_{(Tlast-\infty)}$ were respectively calculated using C_n/λ_z and $t_n C_n/\lambda_z + C_n/\lambda_z{}^2$, where C_n is the last quantifiable concentration. Terminal-phase rate constant (λ_z) was calculated by the regression of the terminal log-linear portion of the plasma concentration curve. Terminal elimination half-life ($t_{1/2}$) was calculated to be $0.693/\lambda_z$. Systemic clearance (CL_t), mean residence time (MRT), and the volume of distribution in the steady state (V_{ss}) were calculated as dose/AUC, AUMC/AUC, and $CL_t \bullet MRT$, respectively. The plasma concentrations of PI polyamides A and B were extrapolated to time zero (C_0). The maximum plasma concentration (C_{max}) of PI polyamide B was directly obtained from the observed data.
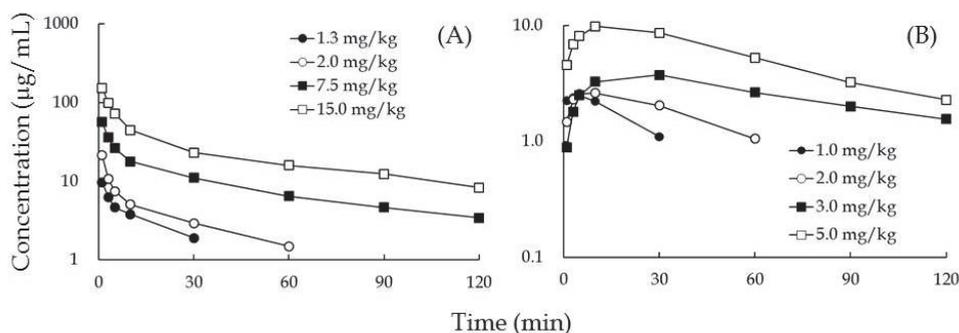
Fig. 6. Mean plasma concentration–time profiles of PI polyamides in rats after intravenous administration. (A) and (B) show PI polyamides A and B.

The pharmacokinetic parameters of PI polyamides A and B obtained in rats using non-compartmental analysis are summarized in Table 3. After the intravenous administration of PI polyamide A at 1.3, 2.0, 7.5, and 15.0 mg/kg, the average $t_{1/2}$, CL_t, and V_{ss} values were in the ranges of 42.3-74.8 min, 4.6-6.4 mL/min/kg, and 244-412 mL/kg, respectively. After the intravenous administration of PI polyamide B at 1.0, 2.0, 3.0, and 5.0 mg/kg, the average $t_{1/2}$, CL_t, and V_{ss} values were in the ranges of 27.5-58.7 min, 7.3-11.9 mL/min/kg, and 407-667 mL/kg, respectively. The CL_t and V_{ss} of PI polyamides A and B showed no significant differences as functions of administration dose. The pharmacokinetics of PI polyamides A and B are linear in the intravenous dose ranges of 1.3-15.0 mg/kg and 1.0-5.0 mg/kg, respectively as revealed by the fact that AUC increased linearly as a function of dose, and CL_t and V_{ss} remained unaltered.

The plasma concentration-time profiles after the intravenous administration of PI polyamide B resembled those after the oral administration. After the intravenous administration of PI polyamide B at 1.0, 2.0, 3.0, and 5.0 mg/kg, C_{max} gradually increased. The concentrations of PI polyamide B in the lungs, liver, heart, kidney and spleen were measured. The mean concentrations of PI polyamide B in the lungs were the highest among those in other tissues, and the mean concentrations 10, 30, and 60 min after injection were 134.7, 97.0, and 73.9 µg/g, respectively. Among various tissues, the concentration of PI polyamide B was observed to be highest in the lungs. The mean lung concentration of PI polyamide B decreased with time.

PI polyamide A

Parameter	Dose			
	1.3 mg/kg	2.0 mg/kg	7.5 mg/kg	15.0 mg/kg
Body weight (kg)	0.267	0.291	0.243	0.26
$t_{1/2}$ (min)	54.8	42.3	74.8	45.3
C_0 (µg/mL)	14.1	22.9	77.1	227.5
AUC (µg min/kg)	259.6	316.8	1528.6	3331.9
Cl (mL/min/kg)	5.6	6.4	5.1	4.6
Vss (mL/kg)	305.8	274.6	411.8	243.7
MRT (min)	68.1	42.6	80.5	54

PI polyamide B

Parameter	Dose			
	1.0 mg/kg	2.0 mg/kg	3.0 mg/kg	5.0 mg/kg
Body weight (kg)	0.313	0.317	0.317	0.317
$t_{1/2}$ (min)	139.1	165.8	207.3	359.3
C_0 (µg/mL)	1.5	4	3.8	4
AUC (µg min/kg)	108.1	205.2	326.8	508.3
Cl (mL/min/kg)	9.9	8.9	9.2	10.3
Vss (mL/kg)	2170.5	1990.1	2602.2	4567
MRT (min)	194.7	222.5	289.7	492.1

Table 3. Mean non-compartmental pharmacokinetic parameters of PI polyamides after intravenous administration at various doses into rats (n = 3).

3.2 Urinary and biliary excretions

Determination of the urinary and biliary excretion rates is crucial for the evaluation of the pharmacokinetics of a drug, because drugs are usually eliminated from the body into urine and/or bile (Ullrich, 1997; van Montfoort et al., 2003). The urinary and biliary excretion rate-time profiles are shown in Figs. 7 and 8, respectively. The urinary excretion rates of PI polyamides A and B showed a linear elimination. The biliary excretion rate of PI polyamide A showed saturation at the early period, while PI polyamide B was not detected in the bile. The cumulative urinary excretion rates of PI polyamides A and B at 48 h were 72.4 ± 11.6 and 4.8 ± 0.5% (mean ± SD, n = 3) of the administered dose, respectively. The cumulative biliary excretion rate of PI polyamide A at 24 h was 4.3 ± 0.4% (n = 4) of the administered dose. These observations indicated that unchanged PI polyamides A and B were slowly eliminated from the body. As observed from the plasma concentration-time profile, it is considered that most of the PI polyamide B remained in the lungs. No peaks of metabolites were detected for all the samples.

The differences in the molecular weights of compounds affect their eliminations (Hirom et al., 1976). The molecular weight thresholds for the excretion of organic cations into rat bile were found to be in the ranges of 200 ± 50 for monovalent organic cations and 500-600 for bivalent organic cations. (Hughes et al., 1973a; b) PI polyamide with a molecular weight of

1422.51 was excreted at 2% into rat urine 24 h after administration and was not detected in rat bile (data not shown). These findings suggested that PI polyamides with high molecular weights tend to be poorly excreted in both rat urine and bile, whereas those with molecular weights less than that of PI polyamide A can be readily eliminated. As described above, the differences in the elimination pathway between PI polyamides A and B may be attributed to the differences in their molecular weights.
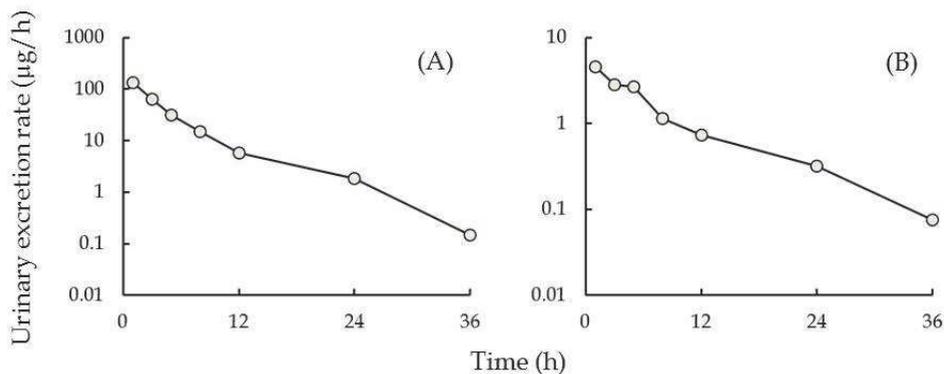
Fig. 7. Urinary excretion rate versus time profile of PI polyamides A (A) and B (B) in rats.
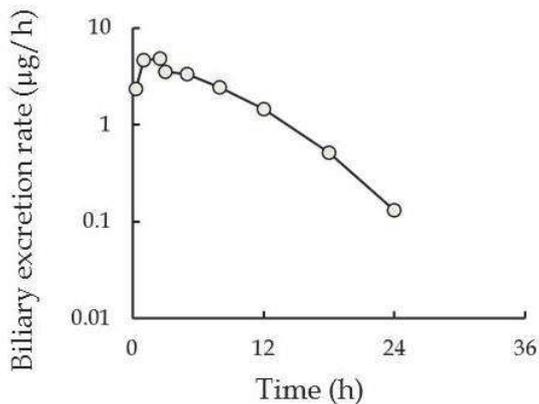
Fig. 8. Biliary excretion rate versus time profile of PI polyamide A in rats.

4. Pharmacokinetic modeling and simulations

4.1 Pharmacokinetic modeling
The plasma concentration-time profiles after the intravenous administration of PI polyamide A was fitted well by a two-compartment model. The estimated pharmacokinetic parameters

using the model are summarized in Table 4. After the intravenous administration of PI polyamide A at 1.3, 2.0, 7.5, and 15.0 mg/kg, the average CL_t and V_{ss} values were in the ranges of 4.9-7.0 mL/min/kg and 245-335 mL/kg, respectively. The CL_t and V_{ss} values estimated using a two-compartment model and a non-compartment model are thought to be identical.

Parameter	Dose			
	1.3 mg/kg	2.0 mg/kg	7.5 mg/kg	15.0 mg/kg
CL_t (mL/min/kg)	5.8	7	5.8	4.9
V_{ss} (mL/kg)	335	250	323	245
V_c (mL/kg)	90.5	89.6	96.6	69.7

Table 4. Estimated pharmacokinetic parameters of PI polyamide A obtained using two-compartment model.

The plasma concentration-time profiles after the intravenous administration of PI polyamide B increased in the early phase and resembled those after the oral administration. The slope of the decline in the lung concentration-time profiles of PI polyamide B was nearly equal to that in the plasma concentration-time profiles of PI polyamide B. To describe the increasing phase of PI polyamide B after the intravenous administration, the lung and plasma concentration-time profiles of PI polyamide B were fitted using a catenary two-compartment model (Fig. 9) (Brown et al., 1981).
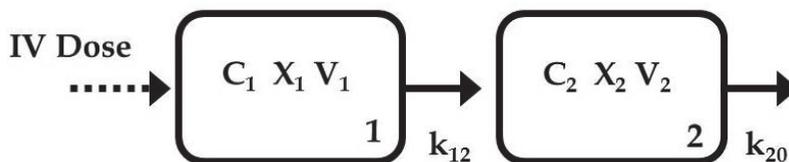
Fig. 9. Pharmacokinetic model of PI polyamide B.

C_1, X_1, and V_1 represent the concentration of PI polyamide B in the lungs, the amount of PI polyamide B in the lungs, and the distribution volume of the lung compartment, respectively. C_2, X_2, and V_2 represent the concentration of PI polyamide B in plasma, the amount of PI polyamide B in plasma, and the distribution volume of the plasma compartment, respectively. The pharmacokinetic parameters were calculated using the NONMEM program.

Figure 10 shows the simulation curves for PI polyamide B based on the catenary two-compartment model. The plasma and lung concentrations were fitted well by the model. The estimated pharmacokinetic parameters after the intravenous administration of PI polyamide B are summarized in Table 5. The estimated coefficients of variation (CV%) were small, the catenary two-compartment model better fitted the concentration-time profile after the intravenous administration of PI polyamide B. The model-estimated clearance (6.8 mL/min/kg) calculated as k_{20} multiplied by V_2 was nearly equal to CL_t (7.3 mL/min/kg). In this study, lung concentrations of first-point were measured at 10 min. It is thought that the

concentration in the lungs immediately after the intravenous administration of PI polyamide B is higher than the calculated value. The early-plasma concentration-time profiles after the intravenous administration of a hairpin polyamide-chlorambucil conjugate, duocarmycin, and nitroglycerin are similar to that of PI polyamide B (Alberts et al., 1998; Chou et al., 2008; Wester et al., 1983) Recently, the biodistribution of a hairpin polyamide-chlorambucil conjugate administered into mice has been reported (Chou et al., 2008). The predominant occupancy of the polyamide-chlorambucil conjugate was observed in the lungs, spleen, small intestine, and pancreas 2 and 24 h after the injection. The concentration of polyamide-chlorambucil conjugate in the lungs at 2 h was higher than that of the polyamide-chlorambucil conjugate at 24 h. These findings are consistent with our results. PI polyamide B is distributed in the aorta and localizes in the nuclei of aortic midlayer smooth muscle (Matsuda et al., 2006). The lungs consist of pulmonary alveoli, which are surrounded by capillary vessels. It has been reported that weak basic drugs accumulate in the lungs and that such accumulation is attributable to lysosomal trapping (MacIntyre et al., 1988; Rodgers et al., 2005). A high concentration of PI polyamide B in the lungs was thought to be caused by PI polyamide B being distributed in capillary vessels of the lungs and by PI polyamide B being a weak base compared with PI polyamide with a molecular weight of 1422.51. It is also conceivable that PI polyamide B accumulated in the lungs owing to its high molecular weight, as suggested in a previous study (Wiseman et al., 2000). From these considerations, the proposed catenary two-compartment model may be applicable to describing PI polyamide B in detail.
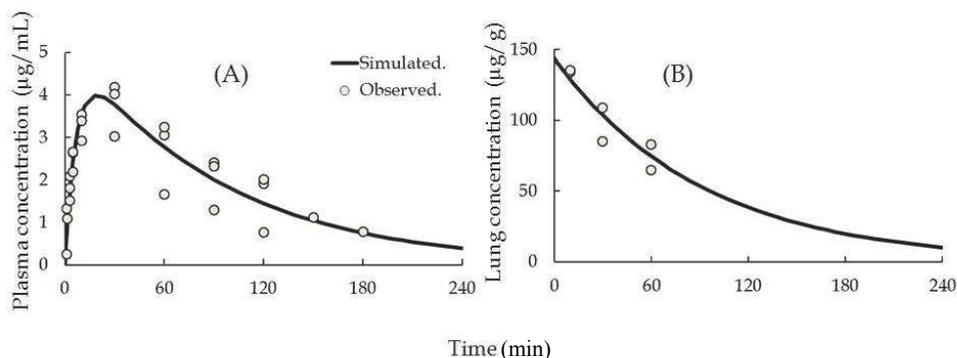
Fig. 10. Model fitted PI polyamide B concentration-time profiles in plasma and lungs. A is plasma concentration–time profiles and B is lung concentration-time profiles. The middle bold line indicates the 50th percentiles for 1000 simulations. Symbols depict the observed data after the intravenous administration of PI polyamide B at 3.0 mg/kg.

4.2 Pharmacokinetic modeling with excretion data in addition to plasma concentration

To predict the plasma concentration-time profile in the elimination phase of PI polyamide A after intravenous administration, two pharmacokinetic models (i.e., one- and two-compartment models with the linear output compartment interpreted as the urine compartment and the non-linear output compartments interpreted as the bile compartment) using the plasma concentration-time profile and cumulative urinary and biliary excretion

Parameter	Estimates
k_{12} (L/min)	0.0109
k_{20} (L/min)	0.1476
V_1 (mL/kg)	20.88
V_2 (mL/kg)	45.86

Table 5. Pharmacokinetic parameters of PI polyamide B from model fitting.
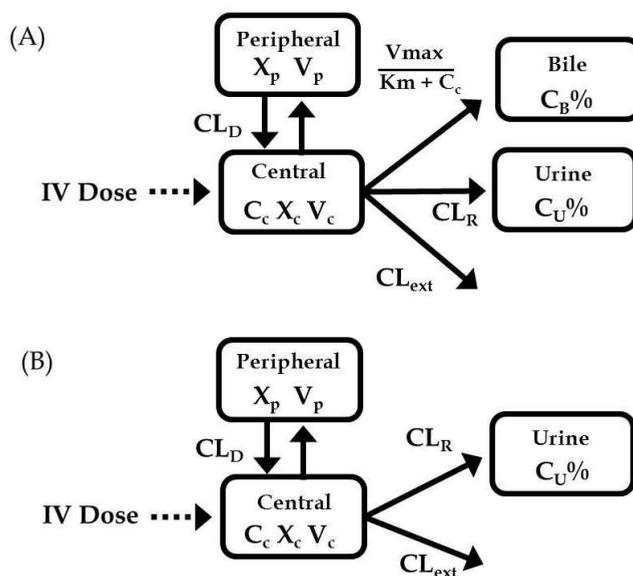
Fig. 11. Scheme of pharmacokinetic model describing the disposition and elimination of PI polyamides A (A) and B (B)

rates of PI polyamide A were tested. A scheme of the two-compartment model, with the linear output compartment interpreted as the urine compartment and the non-linear output compartment interpreted as the bile compartment, is shown in Fig. 11A.

X and V are the amount and volume of distribution in the corresponding compartments designated by the subscripts C, P, U, and B representing central, peripheral, urine, and bile compartments, respectively. CL_D is the distribution clearance, CL_R is the renal clearance, CL_{ext} is the clearance excluding renal and biliary clearances, V_{MAX} is the maximum velocity for excretion into bile, and Km is the Michaelis constant for excretion into bile. Cc represents the plasma concentration of PI polyamide A. $C_U\%$ and $C_B\%$ represent the cumulative urinary and biliary excretion rates (percentage of administered dose), respectively.

The residual error model of the plasma concentration was assumed to be the proportional error model because the plasma concentration was measured by HPLC. The model of the cumulative urinary and biliary excretions was assumed to be the additive error model

because the percentage of the administered dose was calculated from the urine and bile concentrations, urine and bile volumes, and administered dose. The choice of model was based on model fitting criteria such as visual inspection of the fitted curves, objective function value of NONMEM (OFV), and CV% of the parameter estimates (Hazra et al., 2007; Matsumoto et al., 2005).

The plasma concentration and cumulative urinary and biliary excretion-time profiles after intravenous administration of PI polyamide A were fitted well by the two-compartment model with the linear output compartment interpreted as the urine compartment and the non-linear output compartment interpreted as the bile compartment (Fig. 12). The 50th percentiles of the model-based prediction for plasma concentrations and cumulative urinary and biliary excretions are presented together with the observed value. To obtain 50th percentiles of the model estimations, 10000 simulations were performed using the estimated model parameters, variability in the estimated parameters, and residual variability of the data. Compared with a one-compartment model using only plasma data, more accurate data can be obtained from the two-compartment model including urine and bile data because PI polyamide A was excreted into urine and bile until at least 36 and 18 h, respectively, after administration. The plasma concentration-time profile in the elimination phase could also be described better using both the linear and non-linear compartments than using plasma data only.
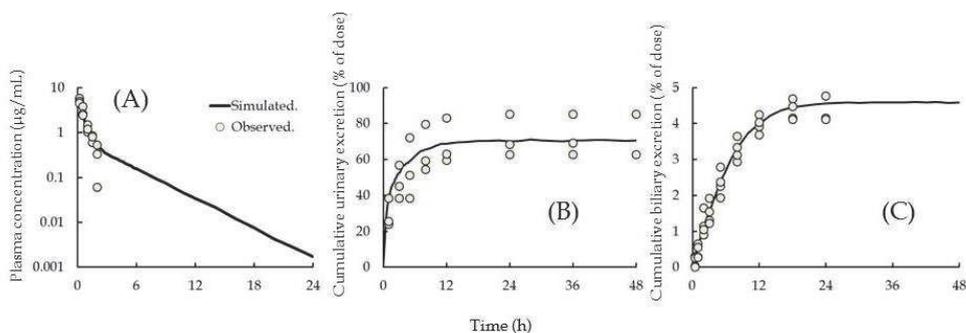
Fig. 12. Plasma concentration–time profile (A), cumulative urinary excretion rate (B), and cumulative biliary excretion rate (C) of PI polyamide A after intravenous administration at 2.0 mg/kg to rats. Each data point represents observed data from three (for plasma and urine) and four rats (for bile). The solid line indicates 50th percentiles from model estimations of 10000 simulations.

To predict the plasma concentration-time profile in the elimination phase of PI polyamide B after intravenous administration, two pharmacokinetic models (i.e., one- and two-compartment models with the linear output compartment interpreted as the urine compartment) using the plasma concentration-time profile and cumulative urinary excretions of PI polyamide B were tested. A scheme of the two-compartment model with the linear output compartment interpreted as the urine compartment is shown in Fig. 11B. The residual error models of the plasma concentration of PI polyamide B were the same as described in the part of PI polyamide A.

The plasma concentration and cumulative urinary excretion-time profiles after intravenous administration of PI polyamide B were fitted well by the two-compartment model with the

linear output compartment interpreted as the urine compartment (Fig. 13). The 50th percentiles of the model-based prediction for plasma concentrations and cumulative urinary excretions are presented together with the observed value. To obtain 50th percentiles of the model estimations, 10000 simulations were performed using the estimated model parameters, variability in the estimated parameters, and residual variability of the data.
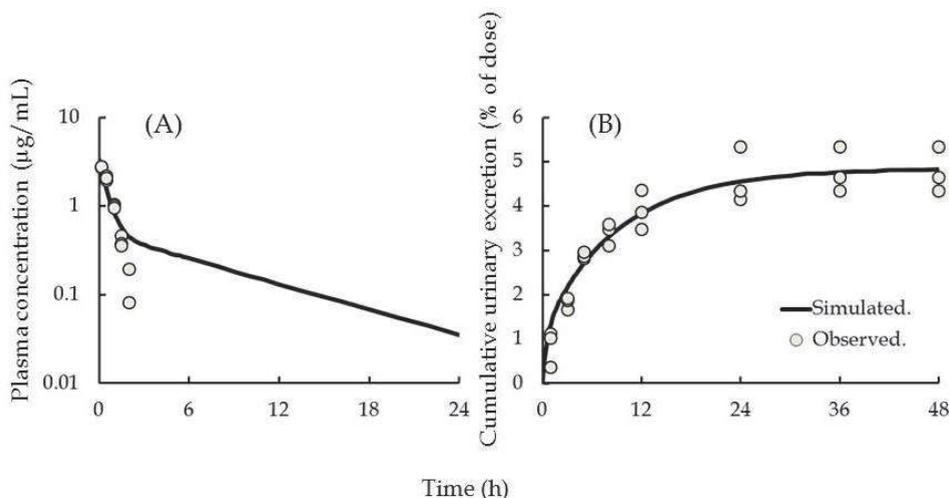
Fig. 13. Plasma concentration–time profile (A) and cumulative urinary excretion (B) of PI polyamide B after intravenous administration at 2.0 mg/kg to rats. Each data point represents observed data from three rats (for plasma and urine). The solid line indicates 50th percentiles from model estimations of 10000 simulations.

To predict the effective dose of PI polyamide B in Dahl-S rats administered at 1 mg every 2 or 3 days for 4 weeks, pharmacokinetic simulations of PI polyamide B were performed using a slightly modified pharmacokinetic model (Nagashima et al., 2009b) by NONMEM program. The average plasma concentrations of PI polyamide B after the administration at 1 mg every 3 and 2 days were 0.18 and 0.28 µg/mL, respectively, which were calculated by the area under the concentration-time curves between 0 and 27 days, divided by 27 days. PI polyamide B did not accumulate following multiple-dose administration.

5. Conclusion

PI polyamides show a remarkable potential for use in non viral gene therapy as many attractive results were obtained. The novel compounds could provide a promising impact on gene therapy for diseases not treatable by current remedies. To obtain the maximum therapeutic effect of the PI polyamide, it is crucial to evaluate the pharmacokinetics of the compounds for designing appropriate dosage regimens. Bioanalytical procedures for PI polyamides A and B were successfully developed and validated by HPLC or LC-MS/MS, and applied to sample assay. The pharmacokinetic profiles of PI polyamides show interesting results, which are thought to be related to their molecular weights (Brown et al.,

1981). It was suggested that the features of various compositions of Py and Im were related to their unique pharmacokinetic profiles. Further examination will be conducted using other PI polyamides that have unique Py and Im combinations for gene therapy.

6. Acknowledgements

7. References

Alberts, S. R.; Erlichman, C.; Reid, J. M.; Sloan, J. A.; Ames, M. M.; Richardson, R. L. & Goldberg, R. M. (1998). Phase I study of the duocarmycin semisyntheticderivative KW-2189 given daily for five days every six weeks. *Clin Cancer Res*, Vol. 4, No. 9, pp. 2111-2117, ISSN 1078-0432 (Print) 1078-0432 (Linking).

Brown, P. H.; Krishnamurthy, G. T.; Bobba, V. V. & Kingston, E. (1981). Radiation dose calculation for Tc-99m HIDA in health and disease. *J Nucl Med*, Vol. 22, No. 2, pp. 177-183, ISSN 0161-5505 (Print) 0161-5505 (Linking).

Chou, C. J.; Farkas, M. E.; Tsai, S. M.; Alvarez, D.; Dervan, P. B. & Gottesfeld, J. M. (2008). Small molecules targeting histone H4 as potential therapeutics for chronic myelogenous leukemia. *Mol Cancer Ther*, Vol. 7, No. 4, pp. 769-778, ISSN 1535-7163 (Print) 1535-7163 (Linking).

Dickinson, L. A.; Gulizia, R. J.; Trauger, J. W.; Baird, E. E.; Mosier, D. E.; Gottesfeld, J. M. & Dervan, P. B. (1998). Inhibition of RNA polymerase II transcription in human cells by synthetic DNA-binding ligands. *Proc Natl Acad Sci U S A*, Vol. 95, No. 22, pp. 12890-12895, ISSN 0027-8424 (Print) 0027-8424 (Linking).

Fukasawa, A.; Aoyama, T.; Nagashima, T.; Fukuda, N.; Ueno, T.; Sugiyama, H.; Nagase, H. & Matsumoto, Y. (2009). Pharmacokinetics of pyrrole-imidazole polyamides after intravenous administration in rat. *Biopharm Drug Dispos*, Vol. 30, No. 2, pp. 81-89, ISSN 1099-081X (Electronic) 0142-2782 (Linking).

Fukasawa, A.; Nagashima, T.; Aoyama, T.; Fukuda, N.; Matsuda, H.; Ueno, T.; Sugiyama, H.; Nagase, H. & Matsumoto, Y. (2007). Optimization and validation of a high-performance liquid chromatographic method with UV detection for the determination of pyrrole-imidazole polyamides in rat plasma. *J Chromatogr B Analyt Technol Biomed Life Sci*, Vol. 859, No. 2, pp. 272-275, ISSN 1570-0232 (Print) 1570-0232 (Linking).

Hazra, A.; Pyszczynski, N.; DuBois, D. C.; Almon, R. R. & Jusko, W. J. (2007). Pharmacokinetics of methylprednisolone after intravenous and intramuscular administration in rats. *Biopharm Drug Dispos*, Vol. 28, No. 6, pp. 263-273, ISSN 0142-2782 (Print) 0142-2782 (Linking).

Hirom, P. C.; Millburn, P. & Smith, R. L. (1976). Bile and urine as complementary pathways for the excretion of foreign organic compounds. *Xenobiotica*, Vol. 6, No. 1, pp. 55-64, ISSN 0049-8254 (Print) 0049-8254 (Linking).

Hughes, R. D.; Millburn, P. & Williams, R. T. (1973a). Biliary excretion of some diquaternary ammonium cations in the rat, guinea pig and rabbit. *Biochem J*, Vol. 136, No. 4, pp. 979-984, ISSN 0264-6021 (Print) 0264-6021 (Linking).

Hughes, R. D.; Millburn, P. & Williams, R. T. (1973b). Molecular weight as a factor in the excretion of monoquaternary ammonium cations in the bile of the rat, rabbit and guinea pig. *Biochem J*, Vol. 136, No. 4, pp. 967-978, ISSN 0264-6021 (Print) 0264-6021 (Linking).

Jang, G. R.; Harris, R. Z. & Lau, D. T. (2001). Pharmacokinetics and its role in small molecule drug discovery research. *Med Res Rev*, Vol. 21, No. 5, pp. 382-396, ISSN 0198-6325 (Print) 0198-6325 (Linking).

MacIntyre, A. C. & Cutler, D. J. (1988). The potential role of lysosomes in tissue distribution of weak bases. *Biopharm Drug Dispos*, Vol. 9, No. 6, pp. 513-526, ISSN 0142-2782 (Print) 0142-2782 (Linking).

Matsuda, H.; Fukuda, N.; Ueno, T.; Katakawa, M.; Wang, X.; Watanabe, T.; Matsui, S.; Aoyama, T.; Saito, K.; Bando, T.; Matsumoto, Y.; Nagase, H.; Matsumoto, K. & Sugiyama, H. (2011). Transcriptional inhibition of progressive renal disease by gene silencing pyrrole-imidazole polyamide targeting of the transforming growth factor-beta1 promoter. *Kidney Int*, Vol. 79, No. 1, pp. 46-56, ISSN 1523-1755 (Electronic) 0085-2538 (Linking).

Matsuda, H.; Fukuda, N.; Ueno, T.; Tahira, Y.; Ayame, H.; Zhang, W.; Bando, T.; Sugiyama, H.; Saito, S.; Matsumoto, K.; Mugishima, H. & Serie, K. (2006). Development of gene silencing pyrrole-imidazole polyamide targeting the TGF-beta1 promoter for treatment of progressive renal diseases. *J Am Soc Nephrol*, Vol. 17, No. 2, pp. 422-432, ISSN 1046-6673 (Print) 1046-6673 (Linking).

Matsumoto, Y.; Fujita, T.; Ishida, Y.; Shimizu, M.; Kakuo, H.; Yamashita, K.; Majima, M. & Kumagai, Y. (2005). Population pharmacokinetic-pharmacodynamic modeling of TF-505 using extension of indirect response model by incorporating a circadian rhythm in healthy volunteers. *Biol Pharm Bull*, Vol. 28, No. 8, pp. 1455-1461, ISSN 0918-6158 (Print) 0918-6158 (Linking).

Murty, M. S. & Sugiyama, H. (2004). Biology of N-methylpyrrole-N-methylimidazole hairpin polyamide. *Biol Pharm Bull*, Vol. 27, No. 4, pp. 468-474, ISSN 0918-6158 (Print) 0918-6158 (Linking).

Nagashima, T.; Aoyama, T.; Fukasawa, A.; Watabe, S.; Fukuda, N.; Ueno, T.; Sugiyama, H.; Nagase, H. & Matsumoto, Y. (2009a). Determination of pyrrole-imidazole polyamide in rat plasma by liquid chromatography-tandem mass spectrometry. *J Chromatogr B Analyt Technol Biomed Life Sci*, Vol. 877, No. 11-12, pp. 1070-1076, ISSN 1873-376X (Electronic) 1570-0232 (Linking).

Nagashima, T.; Aoyama, T.; Yokoe, T.; Fukasawa, A.; Fukuda, N.; Ueno, T.; Sugiyama, H.; Nagase, H. & Matsumoto, Y. (2009b). Pharmacokinetic modeling and prediction of plasma pyrrole-imidazole polyamide concentration in rats using simultaneous

urinary and biliary excretion data. *Biol Pharm Bull*, Vol. 32, No. 5, pp. 921-927, ISSN 0918-6158 (Print) 0918-6158 (Linking).

Pilch, D. S.; Poklar, N.; Gelfand, C. A.; Law, S. M.; Breslauer, K. J.; Baird, E. E. & Dervan, P. B. (1996). Binding of a hairpin polyamide in the minor groove of DNA: sequence-specific enthalpic discrimination. *Proc Natl Acad Sci U S A*, Vol. 93, No. 16, pp. 8306-8311, ISSN 0027-8424 (Print) 0027-8424 (Linking).

Rodgers, T.; Leahy, D. & Rowland, M. (2005). Tissue distribution of basic drugs: accounting for enantiomeric, compound and regional differences amongst beta-blocking drugs in rat. *J Pharm Sci*, Vol. 94, No. 6, pp. 1237-1248, ISSN 0022-3549 (Print) 0022-3549 (Linking).

Takahashi, T.; Asami, Y.; Kitamura, E.; Suzuki, T.; Wang, X.; Igarashi, J.; Morohashi, A.; Shinojima, Y.; Kanou, H.; Saito, K.; Takasu, T.; Nagase, H.; Harada, Y.; Kuroda, K.; Watanabe, T.; Kumamoto, S.; Aoyama, T.; Matsumoto, Y.; Bando, T.; Sugiyama, H.; Yoshida-Noro, C.; Fukuda, N. & Hayashi, N. (2008). Development of pyrrole-imidazole polyamide for specific regulation of human aurora kinase-A and -B gene expression. *Chem Biol*, Vol. 15, No. 8, pp. 829-841, ISSN 1074-5521 (Print) 1074-5521 (Linking).

Tao, Z. F.; Fujiwara, T.; Saito, I. & Sugiyama, H. (1999). Sequence-specific alkylation of DNA by duocarmycin A and its novel derivatives bearing PY/IM polyamides. *Nucleosides Nucleotides*, Vol. 18, No. 6-7, pp. 1615-1616, ISSN 0732-8311 (Print) 0732-8311 (Linking).

Trauger, J. W.; Baird, E. E. & Dervan, P. B. (1996). Recognition of DNA by designed ligands at subnanomolar concentrations. *Nature*, Vol. 382, No. 6591, pp. 559-561, ISSN 0028-0836 (Print) 0028-0836 (Linking).

Ueno, T.; Fukuda, N.; Tsunemi, A.; Yao, E. H.; Matsuda, H.; Tahira, K.; Matsumoto, T.; Matsumoto, K.; Matsumoto, Y.; Nagase, H.; Sugiyama, H. & Sawamura, T. (2009). A novel gene silencer, pyrrole-imidazole polyamide targeting human lectin-like oxidized low-density lipoprotein receptor-1 gene improves endothelial cell function. *J Hypertens*, Vol. 27, No. 3, pp. 508-516, ISSN 1473-5598 (Electronic) 0263-6352 (Linking).

Ullrich, K. J. (1997). Renal transporters for organic anions and organic cations. Structural requirements for substrates. *J Membr Biol*, Vol. 158, No. 2, pp. 95-107, ISSN 0022-2631 (Print) 0022-2631 (Linking).

van Montfoort, J. E.; Hagenbuch, B.; Groothuis, G. M.; Koepsell, H.; Meier, P. J. & Meijer, D. K. (2003). Drug uptake systems in liver and kidney. *Curr Drug Metab*, Vol. 4, No. 3, pp. 185-211, ISSN 1389-2002 (Print) 1389-2002 (Linking).

Wester, R. C.; Noonan, P. K.; Smeach, S. & Kosobud, L. (1983). Pharmacokinetics and bioavailability of intravenous and topical nitroglycerin in the rhesus monkey: estimate of percutaneous first-pass metabolism. *J Pharm Sci*, Vol. 72, No. 7, pp. 745-748, ISSN 0022-3549 (Print) 0022-3549 (Linking).

White, S.; Baird, E. E. & Dervan, P. B. (1997). On the pairing rules for recognition in the minor groove of DNA by pyrrole-imidazole polyamides. *Chem Biol*, Vol. 4, No. 8, pp. 569-578, ISSN 1074-5521 (Print) 1074-5521 (Linking).

Wieser, M. (2006). Atomic weights of the elements 2005. *Pure Appl. Chem.*, Vol. 78, No. 11, pp. 2051-2066,

Wiseman, G. A.; White, C. A.; Stabin, M.; Dunn, W. L.; Erwin, W.; Dahlbom, M.; Raubitschek, A.; Karvelis, K.; Schultheiss, T.; Witzig, T. E.; Belanger, R.; Spies, S.; Silverman, D. H.; Berlfein, J. R.; Ding, E. & Grillo-Lopez, A. J. (2000). Phase I/II 90Y-Zevalin (yttrium-90 ibritumomab tiuxetan, IDEC-Y2B8) radioimmunotherapy dosimetry results in relapsed or refractory non-Hodgkin's lymphoma. *Eur J Nucl Med*, Vol. 27, No. 7, pp. 766-777, ISSN 0340-6997 (Print) 0340-6997 (Linking).
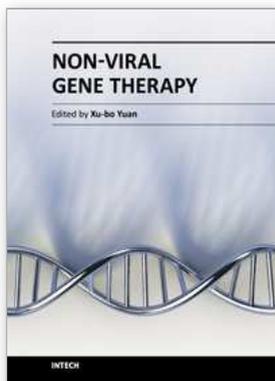
Non-Viral Gene Therapy

Edited by Prof. Xubo Yuan

ISBN 978-953-307-538-9

Hard cover, 696 pages

Publisher InTech

Published online 07, November, 2011

Published in print edition November, 2011

This book focuses on recent advancement of gene delivery systems research. With the multidisciplinary contribution in gene delivery, the book covers several aspects in the gene therapy development: various gene delivery systems, methods to enhance delivery, materials with modification and multifunction for the tumor or tissue targeting. This book will help molecular biologists gain a basic knowledge of gene delivery vehicles, while drug delivery scientist will better understand DNA, molecular biology, and DNA manipulation.

INTECH

open science | open minds